Int. J. Electrochem. Sci., 12 **(2017)** 466 – 474, doi: 10.20964/2017.01.42

International Journal of
ELECTROCHEMICAL
SCIENCE
www.electrochemsci.org

Short Communication

Microwave Synthesis of Reduced Graphene Oxide-Supported Platinum Nanocomposite with High Electrocatalytic Activity for Methanol Oxidation

Jiliang Xie[1,2,*] *Xujie Yang*[1] *Xingyou Xu*[1,3] *and Chao Yang*[4]

[1] Chemical Engineering Institute, Nanjing University of Science and Technology Nanjing, 210094, P.R. China
[2] Jiangsu Marine Resources Development Research Institute, Lianyungang 222001, P.R. China
[3] School of Chemical Engineering, Huaihai Institute of Technology, Lianyungang 222005, P.R. China
[4] Institute of Process Engineering,Chinese Academy of Sciences, Beijing, 100190, P.R. China
[*]E-mail: jiliangxie_nust3@foxmail.com

Received: 15 October 2016 / *Accepted:* 22 November 2016 / *Published:* 12 December 2016

Pt/RGO electrocatalyst was successfully prepared by the deposition of platinum nanoparticles on the surface of reduced graphene oxide with a rapid and environment-friendly microwave-assisted polyol method. The electrochemical activity of as-synthesized Pt/RGO for methanol electrooxidation was investigated in detail. As can be seen from certain values including diffusion coefficient, current density of forward oxidation peak and ratio of the current density of forward peak to reverse peak, the electrooxidation performance of Pt/RGO was superior to that of Pt/C and Pt/graphite catalysts. For example, the current density of forward oxidation peak obtained with Pt/RGO catalyst for methanol oxidation was 18.5 mA/cm^2, which was higher than that obtained with Pt/C catalyst (9.65 mA/cm^2).

Keywords: Graphene; Platinum; Methanol oxidation; Electrocatalysis; Microwave synthesis

1. INTRODUCTION

The controllable synthesis of novel hybrid nanostructures with unique functionality by the assembly of different nanomaterials is one of the most important but challenging processes in nanoscience [1-3]. Typically, hybrid nanostructures are expected to possess the advantages of all consisting nanomaterials. In particular, the hybrid nanostructure that contains carbon and metal has demonstrated promising potential as electrode materials in various fields such as biosenser and fuel cells [4-6].

Fuel cell, a device that converts chemical energy into electricity by the catalytic conversion of a fuel (e.g., hydrogen and methanol), has many advantages such as high efficiency and virtually absence of pollutants [7-10]. However, certain technological barriers are still required to be solved in order to achieve commercial applications. The CO poisoning of platinum (Pt) electrode belongs to one of these barriers. Specifically, CO can occupy the active sites of Pt and further impede the oxidation of fuel. CO poisoning is particularly serious for direct methanol fuel cells (DMFCs) owing to the permanent existence of CO as an intermediate in the oxidation process of methanol. The incorporation of other oxophilic elements including Pd, Ni, Ru and Au into Pt is verified to be an effective method to reduce the effect of CO poisoning [11-15]. The improved tolerance of Pt alloy to CO can be explained by the following two mechanisms. The bifunctional mechanism model assumed that the oxidation of CO was promoted by the adsorbed OH species at platinum/ruthenium edge which was generated by water dissociation [16-19]. And the intrinsic or ligand mechanism assumed that the affinity of Pt for CO was reduced owing to the change of electronic structure of Pt by neighboring ruthenium. Unfortunately, the incorporation of additional metal elements makes DMFC uneconomical despite its effect on reducing CO poisoning. Therefore, to develop more cost-effective methods is highly demanded.

An effective method to enhance the electrocatalytic activity is the employment of carbon as support, which is propitious to the dispersion of metal catalyst and promotion of electron and mass transfer kinetics as well. Prior to the catalyst deposition, the oxides on the surface of carbon supports was found to have the ability to increase the electrocatalytic activity of carbon for methanol oxidation, owing to the improved accessibility of methanol to the surface of carbon support [20-23]. Besides, the particle growth was limited and thus the dispersion of metal nanoparticles was improved due to the oxygen functional groups as nucleation sites, which effectively enhanced the stability of supported catalysts. However, the influence of oxygen-containing functional groups on the resistance to CO poisoning is still short of cognition. Unfortunately, very few people have studied this issue. In addition, oxidized supports should be prevented owing to the low conductivity.

Graphene, a promising form of carbon, possesses many advantages such as extremely high specific surface area, excellent thermal/chemical stability and exceptional thermal/electrical conductivity as well. The electron transport can be greatly improved by the deposition of catalyst nanoparticles (NPs) on the two-dimensional graphene support, which inaugurate a new area in the design of next generation catalysts [24-26]. Currently, the chemical exfoliation of graphite by strong acids is the gram-scale production method of graphene. Many oxygen-containing functional groups including epoxide, carboxyl, keto and hydroxyl were generated at the planes and edges of graphene layers through the oxidation procedure. The resulting graphene oxide (GO) is in poor electrical conductivity, which can be greatly improved by reduction process with reducing agents.

In this study, a one-step environment-friendly microwave-assisted polyol process (MWAPP) was employed to prepare Pt/RGO electrocatalysts. The applied polyol ethylene glycol (EG) can be not only dispersing agent but also reductive agent, which effectively promoted the synthesis of Pt nanocrystals on the surface of RGO. Microwaves heating method outperforms many other heating methods with regard to heating rate, uniformity, simplicity and energy efficiency. The performance such as catalytic activity, stability and resistance to CO poisoning of constructed RGO-supported Pt

nanocrystals outperforms the commercial carbon-supported Pt electrocatalysts (Pt/C) when applied in methanol oxidation reaction (MOR).

2. EXPERIMENTS

2.1. Synthesis

The synthetic method for carbon nanotube-supported Pt catalyst was employed herein for the preparation of graphene-supported Pt owing to the similar structure between graphene and carbon nanotubes [27]. Firstly, Hummers method was used for the preparation of graphene oxide from a solution of graphite [28]. The obtained graphene oxide powder (100 mg) was added into ethylene glycol (EG) solution (10 mL) and then the solution was dealt with sonication for 30 min. Then 1.5 mL of EG solution containing hexachloroplatinic acid (H_2PtCl_6) with the concentration of 7.4 mg/mL was mixed into the above-obtained graphene oxide solution and the mixture was stirred for 2 h. Subsequently, the sodium hydroxide EG solution with the concentration of 2.5 M was applied to adjust the pH of the mixed solution to 13.0. Subsequently, the mixed solution was refluxed at 100 °C for 5 h with the protection of argon. Finally, the product was filtered from the solution, rinsed with water and then dried at 60 °C in oven overnight.

2.2. Characterization

The SEM images of Pt nanoparticles, catalyst supports and the composite of Pt nanoparticles and catalyst supports were obtained with scanning electron microscope (SEM, JEOL JSM-840A) and field emission scanning electron microscope (FESEM, FEI Quanta 200) that is equipped with X-ray energy dispersive spectrometer (EDS, Oxford INCA 250 silicon).

2.3. Electrocatalytic activity measurements

A CHI 660A electrochemical work station with the conventional three electrode cell (electrocatalysts modified glassy carbon, Ag/AgCl and Pt wire as working, reference and counter electrode, respectively) was employed for the investigation of electrocatalytic activity of as-synthesized electrocatalysts. The working electrode was synthesized with the following steps: catalyst powder (4 mg) was firstly dispersed uniformly in ethanol (2 mL) and the mixed solution was dealt with sonication for 30 min, then the above-obtained suspension (30 μL) and Nafion solution (10 μL) with the concentration of 5 wt.% were dropped onto glassy carbon electrode, and the electrode was finally dried at 25 ^{o}C for 15 min. The addition of Nafion is highly important to the well combination of catalyst membrane and electrode surface owing to its adhesive interaction. Before the electrochemical experiments, the electrolyte was degased with nitrogen for 20 min. In order to investigate the performance of Pt/graphene, Pt/graphite and Pt/carbon black electrocatalysts for the electrocatalytic

oxidation of methanol, cyclic voltammetry was employed with the mixture of CH_3OH (1M) and H_2SO_4 (0.5 M) solution ss electrolyte and -0.3-1.0 V as applied potential.

The diameter of 3 mm was applied, of which the area was used for the calculation of electrical current density. All electrocatalysts (Pt/graphene, Pt/graphite and Pt/carbon black) were prepared for three times at exactly the same conditions for the sake of investigating reproducibility.

3. RESULTS AND DISCUSSION

As can be seen from the SEM images of graphene, graphite and carbon black (Fig. 1), different morphologies were observed. Graphene sheets are crumpled with the size ranging from several hundred nanometer to tens of micrometer. Graphite is in platelet shape with the size in the following range 5-50 μm. Besides, the dimension of carbon black ranges from 20 to 80 nm. The morphological difference of three supports is propitious to well understand the effect of support morphology on its electrocatalytic performance for methanol oxidation.

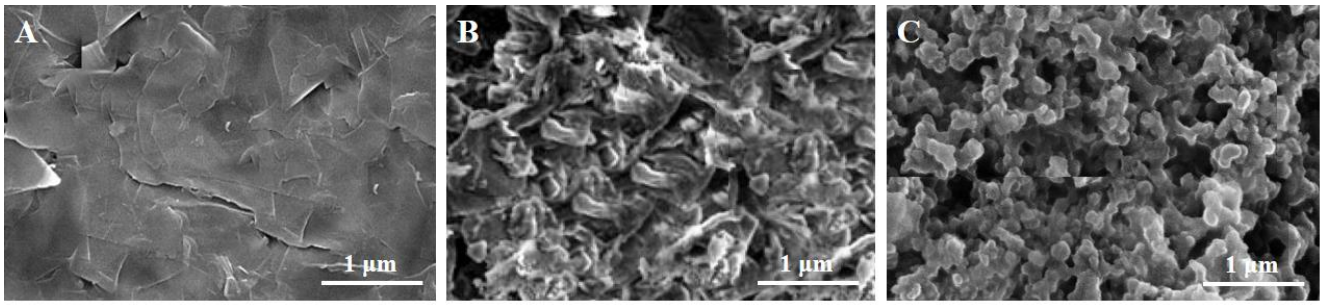

Figure 1. SEM images of catalyst supports: (A) graphene, (B) graphite and (C) carbon black.

In addition to the significant role in the reduction process of graphene oxide, metallic nanoparticles have been demonstrated to be able to hinder the restacking of RGO (reduced graphene oxide) by means of forming the composite of metallic nanoparticles and RGO as well [21-22]. As shown from the typical BSE image of Pt/RGO (Fig. 2A), Pt nanoparticles are the bright ones with the dimension of less than 10 nm which is hard to be detected in the SEM image. The formation of Pt on the surface of graphene sheets was further affirmed by EDS spectrum (Fig. 2B). The reduction of graphene oxide to graphene is assumed to be incomplete due to the observable oxygen signal. Besides, sodium signal which could be ascribed to sodium hydroxide or sodium nitrate used in the synthesis of the composite of metallic nanoparticles and RGO was also observed.

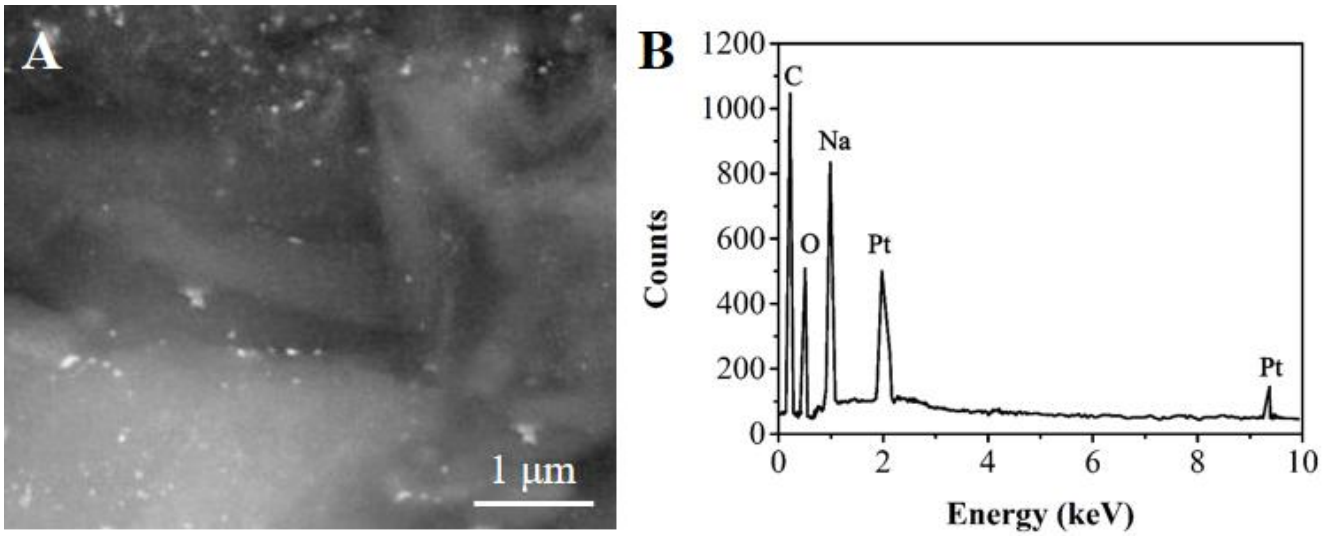

Figure 2. (A) Z-contrast BSE image and (B) EDS spectrum of Pt/RGO.

XRD spectra of GO, Pt/RGOs and commercial Pt/carbon black (Pt/C) catalyst were shown in Fig. 3. A new 002 peak (2θ = 11.1°, *d*-spacing=0.78 nm) in place of graphite peak (002) at 2θ = 26.2° with *d*-spacing of 3.35 Å was found in the XRD pattern of GO, indicating the successful preparation of GO. The *d*-spacing of GO sheets was found to be increased owing to the roughness of graphene sheet caused by the existence of abundant O-moieties on the surface. As can be seen from the XRD pattern of Pt/RGOs, the intensity of GO peak was suppressed and the conjugated graphene network (sp^2 carbon) was re-established, suggesting the successful reduction of GO to RGO. Besides, the carbon peak (002) of Pt/RGO became broader with the FWHM of 4.94 and 4.72°, indicating the existence of various oxidation states. In addition, the diffraction peaks at 2θ = 39.3, 46.0, 67.3° and 81.24° belong to the (111), (200), (220) and (311) crystalline planes of Pt in fcc structure, respectively, suggesting the formation of Pt NPs crystallinity.

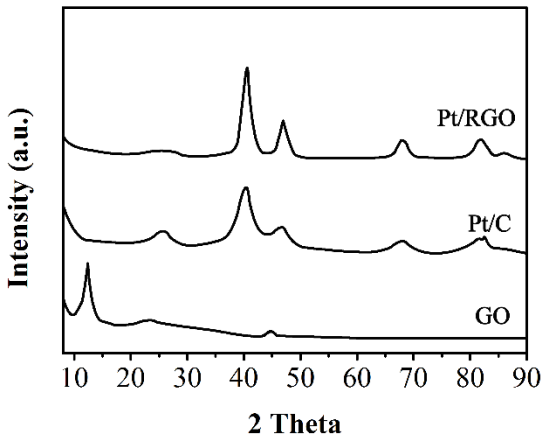

Figure 3. XRD spectra of GO, Pt/RGO hybrids and Pt/C.

As shown in XPS spectrum of C1s for Pt/RGO (Fig. 4A), new sp^2 C-C bonds were formed and the amount of oxygen moieties decreased, leading to the greatly increase of C/O ratio. Besides, the intensity of C-C peak increased accompanied with remarkable decrease of overlapping peaks at 285.5-289.0 eV. All the above-mentioned phenomena indicated that RGO was successfully prepared by the reduction of GO. In contrast to the Pt/C with very small amounts of hydroxyl groups, certain amount of O-moieties were still observed in Pt/RGO hybrids despite that the MWPP reduction would reduce the amount of O-moieties.

As shown in Pt 4f spectrum of Pt/RGO (Fig. 4B), doublets of Pt $4f^{5/2}$ and Pt $4f^{7/2}$ were observed, indicating that the existence of Pt^0, Pt^{2+} and Pt^{4+} oxidation states. It is worth noting that a certain amount of Pt^0 existed despite the existence of a large amount of oxygen-containing functional groups in GO.

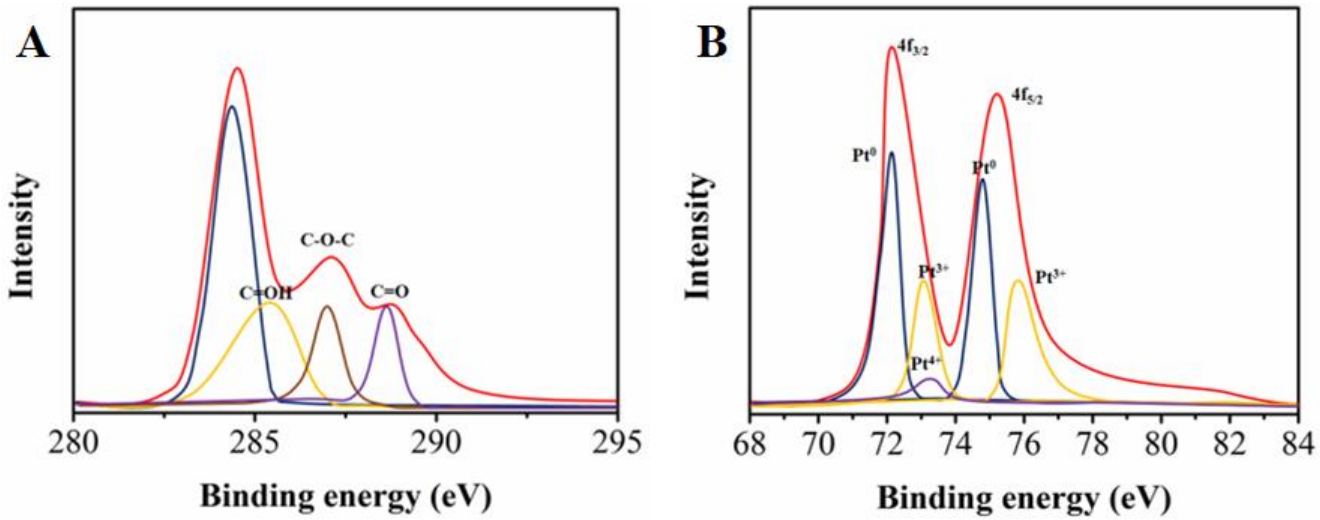

Figure 4. High-resolution XPS spectra of (A) C1s and (B) Pt 4f for Pt/RGO hybrids.

Cyclic voltammetry experiment was used for the investigation of electrocatalytic performance of Pt/RGO, Pt/C and Pt/graphite electrocatalysts for methanol oxidation. Specifically, the experimental parameters are as follows: the mixture of CH_3OH (1 M) and H_2SO_4 (0.5 M) as electrolyte, 50 mV/s as scan rate and −0.3 to +1.0 V as applied potential range. It was found that the voltammograms obtained on each catalyst were similar and the recorded data became stable after fifth cycle. Fig. 5 showed the voltammograms recorded after fifth cycle. The electrocatalytic performance of different electrocatalysts for methanol oxidation was compared in detail. Table 1 presented the oxidation potential and peak current density and the ratio of forward to reverse peak current density.

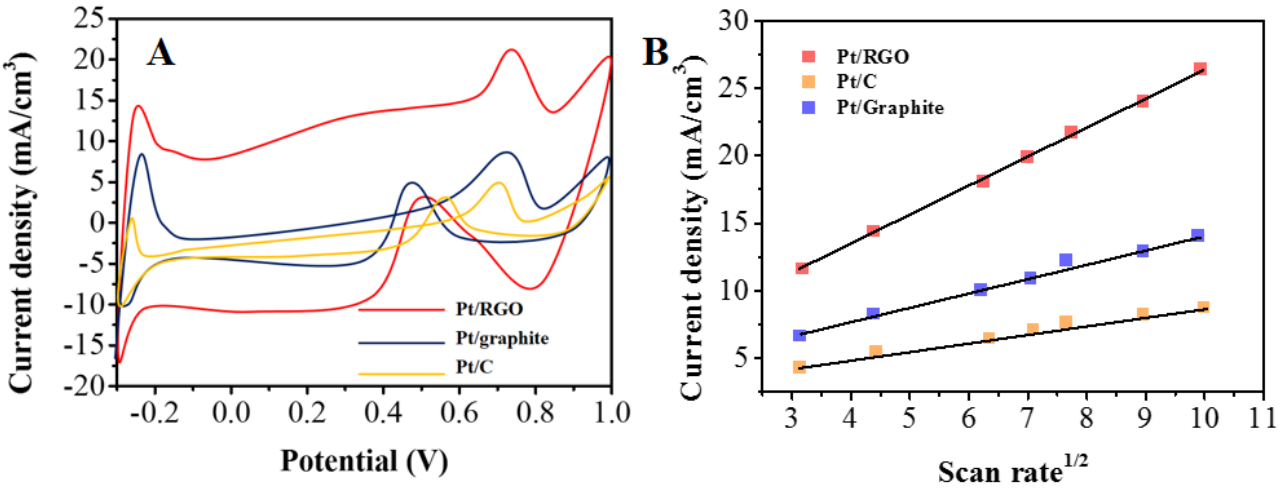

Figure 5. (A) Cyclic voltammograms of Pt/RGO, Pt/C and Pt/graphite electrocatalysts for methanol oxidation. (B) Peak current density in function of scan rate.

Table 1. Comparison of electrocatalytic performance of Pt/RGO, Pt/C and Pt/graphite for methanol oxidation.

Electrode	Forward sweep		Reverse sweep		IF/IR Ratio
	I_F (mA/cm^2)	E (V)	I_R (mA/cm^2)	E (V)	
Pt/RGO	18.5	0.65	3.05	0.47	6.51
Pt/C	9.65	0.59	6.85	0.42	1.40
Pt/graphite	6.45	0.58	6.20	0.40	1.02

Both activity for methanol oxidation and tolerance to CO of Pt/RGO electrocatalysts were better than that of Pt/C and Pt/graphite electrocatalysts. In the forward scanning process, the current showed a slow increase at low potentials but a sharp increase at potentials higher than 0.5 V. The oxidation process was found to occur at 0.65 V. The peak current density obtained with Pt/RGO catalyst was 18.5 mA/cm^2, which was nearly three times than that obtained with Pt/C and Pt/graphite electrocatalysts. As we all know, the amount of methanol oxidized was directly proportional to peak current density. The better electrocatalytic activity of Pt/RGO indicated that graphene contributed to the enhancement of the activity of Pt for methanol oxidation. In the reverse scanning process, an oxidation peak at 0.46 V was observed which could be ascribed to the oxidation reaction of CO and other carbon species that formed on the electrode. And the reverse peak current density obtained with Pt/RGO catalyst was 3.05 mA/cm^2, which was much lower than that obtained with carbon back (7.85 mA/cm^2) and graphite (6.20 mA/cm^2) -supported Pt nanoparticles. Typically, the tolerance of catalyst to CO and other carbon species can be described with the ratio of forward anodic peak current density (I_F) to reverse anodic peak current density (I_R). The I_F/I_R of Pt/RGO catalyst was 6.51, much higher than that of Pt/C (1.40) and Pt/graphite (1.42), indicating that the electrocatalytic performance of Pt/RGO catalyst has more effect on methanol other than carbon dioxide. A possible bifunctional

effect between Pt nanoparticles and remaining oxygenated groups is similar with the commonly accepted bifunctional mechanism of methanol electro-oxidation between Pt and Ru [29, 30].

I_F was found to be proportional to the square root of scan rate for all Pt/RGO, Pt/C and Pt/graphite catalysts, demonstrating that the oxidation of methanol was diffusion-controlled. The methanol diffusion coefficient of RGO was higher than that of C and graphite as evidenced by the larger slope of Pt/RGO than Pt/C and Pt/graphite. The result also show that the forward peak current density increases initially and remains stable, and then gradually decreases with successive scans. The Pt/RGO catalyst retains 100% of the initial current density, even after 1000 cycles. This performance is better than the reported other graphene-Pt systems, in which the current density decays at a much faster rate within 15–20 cycles due to the formation and gradual accumulation of intermediates such as CO_{ads}, CH_3OH_{ads}, and CHO_{ads} on the catalyst surface during the methanol oxidation reaction, significantly poisoning the Pt NPs for methanol oxidation [31, 32].

All the experimental results mentioned above demonstrated that the electrocatalytic performance of Pt/RGO catalyst was better than that of Pt/C and Pt/graphite for methanol oxidation. The superior electrocatalytic activity of Pt/RGO can be ascribed to exceptional electrical conductivity and large BET surface area and of graphene sheets, which are highly important to the exploitation of novel catalyst supports for direct methanol fuel cells.

4. CONCLUSIONS

In conclusion, the Pt/RGO composite was successfully prepared and then applied as catalyst for methanol oxidation. Compared with Pt/C and Pt/graphite catalysts, Pt/RGO electrocatalyst possessed higher electrochemical activity for methanol oxidation and better CO tolerance. Graphene sheets have demonstrated to have promising potentials as catalyst supports in various applications such as methanol fuel cell. Certainly, the industrial application is contingent upon the exploitation of graphene sheet production in large scale.

References

1. T. Prabhakaran and J. Hemalatha, *Ceram. Int.*, 40 (2014) 3315
2. G. Liu, M.M. Attallah, Y. Jiang and T.W. Button, *Ceram. Int.*, 40 (2014) 14405
3. J. Find, S.C. Emerson and I.M.K.W.R. Moser, *Universitat De València*, 61 (2015) 272
4. M.L. Yola, T. Eren and N. Atar, *Sensors & Actuators B Chemical*, 195 (2014) 28
5. X. Liu, N. Zhang, T. Bing and D. Shangguan, *Anal. Chem.*, 86 (2014) 2289
6. M.R. Joya, *Fullerenes Nanotubes & Carbon Nanostructures*, 23 (2015) 566
7. J. Uribe-Godínez, V. García-Montalvo and O. Jiménez-Sandoval, *International Journal of Hydrogen Energy*, 39 (2014) 9121
8. F. Yang, F. Li, Y. Wang, X. Chen, D. Xia and J. Liu, *Journal of Molecular Catalysis A Chemical*, 400 (2015) 7
9. Z. Yin, Y. Zhang, K. Chen, J. Li, W. Li, P. Tang, H. Zhao, Q. Zhu, X. Bao and D. Ma, *Scientific reports*, 4 (2014)
10. Z. Cui, H. Chen, M. Zhao, D. Marshall, Y. Yu, H. Abruña and F.J. Disalvo, *Journal of the*

American Chemical Society, 136 (2014) 10206
11. S.K. Koehn, S. Gronert and J.T. Aldajaei, *Organic Letters*, 12 (2010) 676
12. M.D. Obradović, U.Č. Lačnjevac, B.M. Babić, P. Ercius, V.R. Radmilović, N.V. Krstajić and S.L. Gojković, *Applied Catalysis B Environmental*, 170-171 (2015) 144
13. H. Xu, M. Zhang, Y. Chen, H. Liu, K. Xu and X. Huang, *Computational & Theoretical Chemistry*, 1061 (2015) 52
14. H.Y. Chou, C.K. Hsieh, M.C. Tsai, Y.H. Wei, T.K. Yeh and C.H. Tsai, *Thin Solid Films*, 584 (2014) 98
15. K. Adach, M. Fijalkowski and J. Skolimowski, *Fullerenes Nanotubes & Carbon Nanostructures*, 23 (2015) 1024
16. C. Hou, J. Jiang, Y. Li, Z. Zhang, C. Zhao and Z. Ke, *Dalton Transactions*, 44 (2015) 16573
17. C.A.A. Monteiro, D. Costa, J.L. Zotin and D. Cardoso, *Fuel*, 160 (2015) 71
18. E. Verabernal, B. Alcántarvázquez, Y. Duan and H. Pfeiffer, *Rsc Advances*, 6 (2016) 2162
19. G.E. Enany, *Fullerenes Nanotubes & Carbon Nanostructures*, 23 (2015) 618
20. H. Duan, Y. Yang, J. Patel, D. Dumbre, S.K. Bhargava, N. Burke, Y. Zhai and P.A. Webley, *Mater. Res. Bull.*, 60 (2014) 232
21. H. Huang and X. Wang, *Journal of Materials Chemistry A*, 2 (2014) 6266
22. V.H. Ramos-Sanchez, D. Brito-Picciotto, R. Gomez-Vargas, D. Chavez-Flores and E. Valenzuela, *Journal of New Materials for Electrochemical Systems*, 17 (2014) 133
23. Y. Zheng, Z. Wang, F. Peng, A. Wang, X. Cai and L. Fu, *Fullerenes Nanotubes & Carbon Nanostructures*, (2015) 00
24. M.A. Nasseri, A. Allahresani and H. Raissi, *Rsc Advances*, 4 (2014) 26087
25. Y. He, N. Zhang, L. Zhang, Q. Gong, M. Yi, W. Wang, H. Qiu and J. Gao, *Mater. Res. Bull.*, 51 (2014) 397
26. L. George, *Fullerenes Nanotubes & Carbon Nanostructures*, 23 (2015) 755
27. Wenzhen Li, Changhai Liang, Weijiang Zhou, Jieshan Qiu, Zhenhua Zhou, A. Gongquan Sun and Q. Xin, *Journal of Physical Chemistry B*, 107 (2003) 149
28. W.S. Hummers and R.E. Offeman, *Journal of the American Chemical Society*, 80 (1958) 1339
29. J. Chen, M. Wang, B. Liu, Z. Fan, K. Cui and Y. Kuang, *J Phys Chem B*, 110 (2006) 11775
30. J. Kua and W.A. Goddard, *Journal of the American Chemical Society*, 121 (1999) 10928
31. J.-D. Qiu, G.-C. Wang, R.-P. Liang, X.-H. Xia and H.-W. Yu, *J Phys Chem C*, 115 (2011) 15639
32. N. Shang, P. Papakonstantinou, P. Wang and S.R.P. Silva, *J Phys Chem C*, 114 (2010) 15837